

## Electrostatic and electromagnetic parallel electron velocity shear instabilities in magnetized plasmas

P. K. Shukla<sup>1</sup>, B. Eliasson<sup>2</sup> and M. Koepke<sup>3</sup>

<sup>1,2</sup>*Institut für Theoretische Physik IV, Fakultät für Physik und Astronomie,  
Ruhr-Universität Bochum, D-44780 Bochum, Germany*

<sup>3</sup>*Department of Physics, West Virginia University, Morgantown, WV 26506-6315, USA*

*Email:* <sup>1</sup>ps@tp4.rub.de, <sup>2</sup>bengt@tp4.rub.de, <sup>3</sup>Mark.Koepke@mail.wvu.edu

### Abstract

We present a theoretical model of parallel electron velocity shear instabilities in magnetized plasmas. Electrostatic instabilities give rise to slowly growing Debye-scale waves that propagate across the magnetic field lines, while electromagnetic instabilities give rise to rapidly growing large-scale waves, primarily propagating at a small angle to the magnetic field lines. The obtained results have relevance for both for laboratory plasma experiments (forthcoming on the WVU Q Machine at the West Virginia University) and for magnetic confinement in fusion devices.

We consider the excitation of low-frequency (in comparison with the electron gyrofrequency  $\omega_{ce} = eB_0/m_e c$ , where  $e$  is the magnitude of the electron charge,  $B_0$  is the strength of the external magnetic field,  $m_e$  is the electron mass, and  $c$  is the speed of light in vacuum) electromagnetic waves by electron parallel flow shear (EPFS) in magnetoplasma [1]. In this study, EPFS is applied by injecting electron streams along the external magnetic field direction in a controlled manner. Here, the ion parallel-flow shear is ignored. We derive linear dispersion relations by using the hydrodynamic equations for the electron fluid

$$\mathbf{v}_{e\perp} \approx \frac{c}{B_0} \hat{\mathbf{z}} \times \nabla \phi - \frac{cT_e}{eB_0 n_0} \hat{\mathbf{z}} \times \nabla n_{e1} + \frac{c}{B_0 \omega_{ce}} \left( \frac{\partial}{\partial t} + u_0 \frac{\partial}{\partial z} \right) \nabla_{\perp} \phi + \frac{u_0}{B_0} \mathbf{B}_{\perp}. \quad (1)$$

Inserting (1) into the linearized electron continuity equation and using the expression for the parallel component of the electron fluid velocity from Ampère's law

$$v_{ez} \approx \frac{c}{4\pi e n_0} \nabla_{\perp}^2 A_z, \quad (2)$$

we obtain

$$\left( \frac{\partial}{\partial t} + u_0 \frac{\partial}{\partial z} \right) \left( n_{e1} + \frac{cn_0}{B_0 \omega_{ce}} \nabla_{\perp}^2 \phi \right) + \frac{c}{4\pi e} \left( \nabla_{\perp}^2 \frac{\partial}{\partial z} + k_e^2 S \frac{\partial}{\partial y} \right) A_z = 0, \quad (3)$$

where  $k_e = \omega_{pe}/c$  is the inverse electron skin depth,  $\omega_{pe} = (4\pi n_0 e^2/m_e)^{1/2}$  is the electron plasma frequency, and  $S = (du_0/dx)/\omega_{ce}$  is the electron shear parameter. The parallel component of the electron equation of motion and Eq. (2) gives

$$\left[ \frac{\partial}{\partial t} - \lambda_e^2 \left( \frac{\partial}{\partial t} + u_0 \frac{\partial}{\partial z} \right) \nabla_{\perp}^2 \right] A_z + c \frac{\partial}{\partial z} \left( \phi - \frac{3T_e n_{e1}}{en_0} \right) + Sc \frac{\partial \phi}{\partial y} = 0, \quad (4)$$

Assuming that  $n_{e1}$  is proportional to  $\exp(-i\omega t + i\mathbf{k} \cdot \mathbf{r})$ , where  $\omega$  is the wave frequency and  $\mathbf{k}$  is the wavevector, we Fourier transform (3) and (4) to obtain

$$\frac{n_{e1}}{n_0} = \frac{k_{\perp}^2 c}{B_0 \omega_{ce}} \left[ 1 - \frac{Q k_z^2 \lambda_e^2 \omega_{ce}^2}{[\omega + (\omega - k_z u_0) b_e](\omega - k_z u_0) - 3Q b_e k_z^2 V_{Te}^2} \right] \phi, \quad (5)$$

where where  $k_{\perp}^2 = k^2 - k_z^2$ ,  $k_z = \hat{\mathbf{z}} \cdot \hat{\mathbf{k}}$ ,  $b_e = k_{\perp}^2 \lambda_e^2$ , and  $Q = (1 + S k_y / k_z) (1 - S k_y / b_e k_z)$ .

We assume a kinetic response for the ions

$$\frac{n_{i1}}{n_0} = - \left[ 1 - \Lambda_0 - \frac{2\omega^2 \Lambda_1}{\omega^2 - \omega_{ci}^2} \right] \frac{e\phi_1}{T_i}, \quad (6)$$

together Poisson's equation,

$$k^2 \phi = 4\pi e (n_{i1} - n_{e1}), \quad (7)$$

to obtain the dispersion relation

$$1 + k^2 \lambda_{Di}^2 + k_{\perp}^2 \rho_a^2 - \Lambda_0 - \frac{2\omega^2 \Lambda_1}{\omega^2 - \omega_{ci}^2} - \frac{Q b_e k_z^2 C_{ea}^2}{[\omega + (\omega - k_z u_0) b_e](\omega - k_z u_0) - 3Q b_e k_z^2 V_{Te}^2} = 0. \quad (8)$$

In the electrostatic limit ( $b_e \gg 1$ ) we have

$$1 + k^2 \lambda_{Di}^2 + k_{\perp}^2 \rho_a^2 - \Lambda_0 - \frac{2\omega^2 \Lambda_1}{\omega^2 - \omega_{ci}^2} - \frac{(1 + S_0) k_z^2 C_{ea}^2}{(\omega - k_z u_0)^2 - 3(1 + S_0) k_z^2 V_{Te}^2} = 0. \quad (9)$$

Equations (8) and (9) are the desired equations for studying the parallel-flow driven electromagnetic and electrostatic modes in a collisionless plasma.

## 1 Numerical results

In order to have a complete picture of instabilities, we now numerically analyze Eq. (8) and (9) for a set of the plasma parameters that are representative of a laboratory experiment. We take  $n_0 = 5 \times 10^{11} \text{ cm}^{-3}$ ,  $B_0 = 2 \text{ kG}$ ,  $T_e = T_i = 0.2 \text{ eV}$ , and  $m_i = 2.3 \times 10^{-22} \text{ gm}$  for Barium ions. For these parameters, we have  $\omega_{pe} = 4 \times 10^{10} \text{ s}^{-1}$ ,  $\omega_{ce} = 3.52 \times 10^{10} \text{ s}^{-1}$ ,  $\omega_{pi} = 7.9 \times 10^7 \text{ s}^{-1}$ ,  $\omega_{ci} = 1.4 \times 10^5 \text{ s}^{-1}$ ,  $\lambda_e = c/\omega_{pe} = 7.5 \text{ cm}$ ,  $V_{Ti} = 4.4 \times 10^5 \text{ cm/s}$ ,  $V_{Te} = 2.2 \times 10^7 \text{ cm/s}$  and  $\alpha = 1.3$ . The electron parallel-flow speed is taken to be  $100V_{Ti}$ . We let  $\omega = \omega_r + i\omega_i$  and plot the real and imaginary parts  $\omega_r/\omega_{pi}$  and  $\omega_i/\omega_{pi}$ , respectively, against  $k_y \lambda_e$  and the ratio  $k_z/k_y$ , where we have made the restriction  $k_x = 0$  so that  $k_{\perp} = k_y$ . The results are displayed in Figs. (1) and (2).

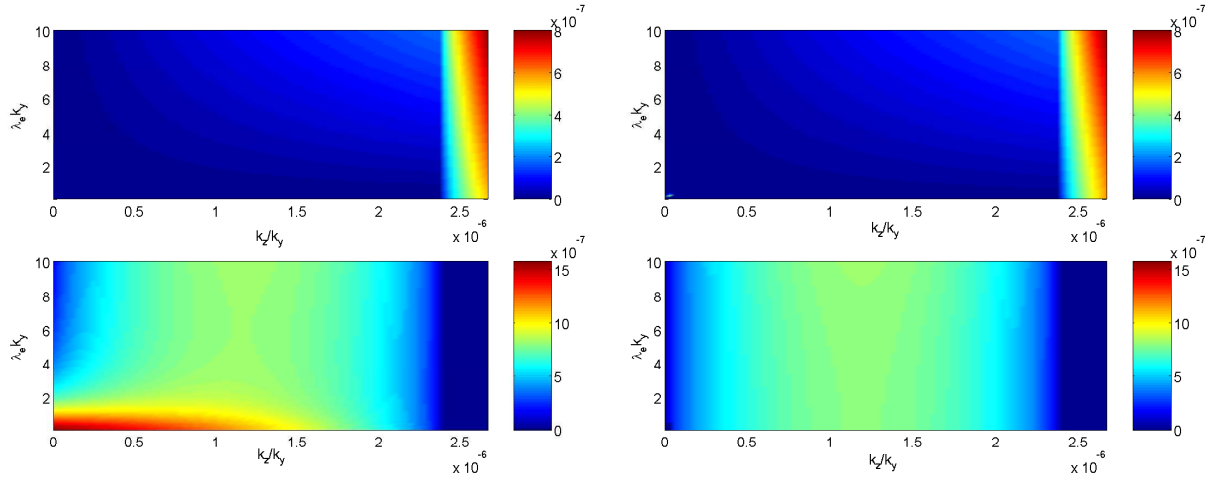


Figure 1: Electromagnetic (left panels) and electrostatic (right panels) shear instability for negative  $S = -2.4 \times 10^{-6}$ . The real part of the normalized (by  $\omega_{pi}$ ) frequency (upper panels) and growth rate (lower panels) versus the normalized wavenumber  $k_y \lambda_e$  and the ratio  $k_z/k_y$ . Both the electromagnetic and electrostatic instabilities occur almost perpendicular to the ambient magnetic field direction, and the region of instability is  $k_z/k_y \lesssim |S|$ . We see that the enhanced growth rate at small wavenumbers in the electromagnetic case (lower left panel) is absent in the electrostatic case (lower right panel). (After Ref. [1].)

Figure 1 shows a comparison between the electromagnetic case governed by Eq. (8) and the electrostatic one governed by Eq. (9). In both cases, we have a weakly growing oscillatory instability almost perpendicular to the magnetic field direction, giving rise to a broad spectrum of waves. The region of instability is here essentially determined by the condition  $(1 + S k_y/k_z) < 0$ , which occurs for  $k_z/k_y < |S|$ . The electromagnetic effects are important for small wavenumbers  $k_y \lambda_e < 1$ , as seen in the lower left panel of Fig. 1, where it gives rise to an enhanced growth rate compared to the one for the electrostatic case shown in the lower right panel of Fig. 1. Going to the regime of positive  $S$  values (or equivalently, keeping  $S$  negative and going to negative values of  $k_z/k_y$ ), shown in Fig. 2, we see that there is a strong and purely growing instability of electromagnetic perturbations almost parallel to the magnetic field direction, with a maximum growth rate for  $k_z/k_y \approx 500$  and  $k_z \lesssim 10^{-2} \lambda_e^{-1}$ . We have varied the electron parallel-flow speed  $u_0$  and the magnitude of the shear parameter  $S$ , while keeping the other parameters constant. We find that the maximum growth rate is almost independent of  $u_0$  (increasing  $u_0$  by a factor ten did not give any visible effect), while the maximum growth rate is proportional to the square root of  $|S|$ . We could not see any impact of the electron temperature on the results for the given parameters, i.e. when we set  $V_{Te} = 0$  the results

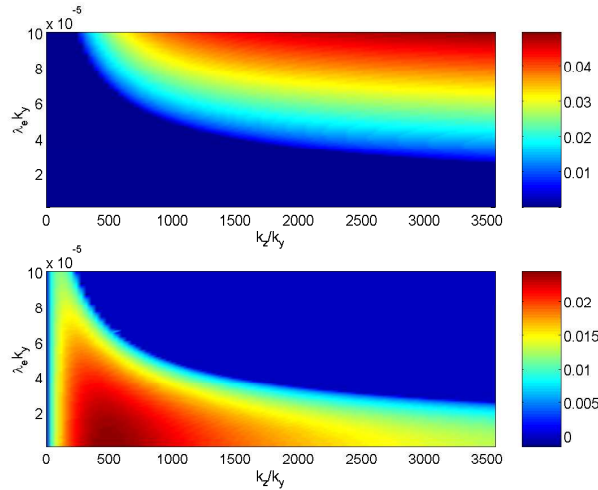


Figure 2: Electromagnetic shear instability for positive  $S = 2.4 \times 10^{-6}$ . The real part of the normalized (by  $\omega_{pi}$ ) frequency (upper panel) and growth rate (lower panel) versus the normalized wavenumber  $k_y \lambda_e$  and the ratio  $k_z/k_y$ . This instability has the strongest growth rate at  $k_z/k_y \approx 500$ , i.e. almost parallel to the external magnetic field direction. The growth rate is much larger than the quasi-perpendicular waves, shown in Fig. 1. (After Ref. [1].)

were more or less unchanged. We have neglected the electron Landau damping in our treatment, which should be included in a more accurate treatment. The instability for positive  $S$  is due to electromagnetic effects and vanishes in the electrostatic limit.

In conclusion, we have examined the growth rates for a few sets of parameters that are representative of forthcoming laboratory experiments at the the WVU Q Machine at the West Virginia University, in which electron velocity shear instabilities will be studied. It is found that the corrections due to electromagnetic effects are important for waves with wavelengths shorter than the electron skin depth. Furthermore, our electromagnetic dispersion relation admits new classes of filamentary instabilities.

**Acknowledgment** This work was partially supported by the Deutsche Forschungsgemeinschaft through the Sonderforschungsbereich 591.

[1] P. K. Shukla, B. Eliasson and M. Koepke, Phys. Plasmas **13**, 052115/1-6 (2006).